

Optimal sensor placement for Spatial Variability Assessment of Structures

Schoefs Franck¹, Bastidas-Arteaga Emilio¹

DOI: <https://doi.org/10.5592/CO/BSHM2017.5.6>

¹ *Université Bretagne Loire, Université de Nantes, GeM, Institute for Research in Civil and Mechanical Engineering, CNRS UMR 6183, Nantes, France,*

E-mail: franck.schoefs@univ-nantes.fr

Abstract. Structural reliability assessment is largely influenced by the spatial variability of material properties or defaults; however, there are still various challenges for their characterization and modeling. Structural Health Monitoring (SHM) could provide useful information in space and time for spatial variability characterization of material properties and mechanical solicitations; nevertheless, this challenge is arduous because of the large number of potential sensor positions of local disruptions/failures. This paper proposes a methodology to optimize the spatial distribution of embedded sensors used for spatial variability assessment of stationary random fields. The optimization criterion relies on the width of the confidence interval of statistics for the characteristics to identify. For sake of simplicity, the paper illustrates the method for one-dimensional problems. The proposed method is applied firstly to a numerical example where several hypothetical structural configurations that could be found in practice are studied. It is finally applied to two case studies (a reinforced concrete beam and a steel wharf) where water content and loss of steel thickness are respectively measured. The results show that the stationary property is useful to deduce the minimum quantity of sensors and their position for a given quality requirement. They also allow us to propose a criterion for defining if regular or non-regular spacing of sensors along the inspection zone is more appropriate depending on the component length and autocorrelation structure of the random field.

Keywords: spatial variability; confidence interval; inspection optimization; stationary field; sensor spacing; Structural Health Monitoring

1 Introduction

Structural serviceability and safety are influenced by the different sources of uncertainty involved during their whole lifetime: material properties, loading, measures, model, deterioration, etc. A probabilistic structural analysis that includes the more influential uncertainties is therefore paramount to minimize both failure risks and design and maintenance costs. Nowadays, there are significant advances in probabilistic modeling at the scale of a single section of the structure. However, various works have demonstrated that the reliability assessment for a given component is largely influenced by the spatial variability of material properties or defaults [Stewart, 2004; Li et al., 2014; Li, 2004; Srivastava, 2012; O'Connor & Kenshel, 2013; Griffiths & Fenton, 2000; Pasqualini et al., 2013]. Although the consideration of spatial variability is essential for proper reliability assessment, there are still various challenges for their characterization and modeling.

Non-Destructive Testing (NDT) and Structural Health Monitoring (SHM) could provide useful information in space and time for spatial variability characterization of material properties and mechanical solicitations. Several studies focused on the use of NDTs for spatial variability characterization at a given time. For example, Nguyen et al [Nguyen et al., 2013, 2014] combined several NDT techniques, kriging and variograms to assess the spatial variability of concrete at different scales (point, local and global). Gomez-Cardenas et al. [Gomez-Cardenas et al., 2015] proposed a two-step approach to optimize the number and position of ultrasound measures required to localize critical zones. More recently, Schoefs et al. (2016) proposed a methodology to find an optimal inspection configuration (number and localization of NDT measures) that minimizes the error of identification of probability distributions for a given quantity of interest (resistance, porosity, water content, etc.) with spatial dependency. SHM could be more useful for characterizing the evolution in time of this spatial variability. Most part of research efforts in SHM have focused on the spatial localization of defects or damage of structural components [Hu et al., 2015; Kuprapha & Warnitchai, 2012]. However, spatial variability characterization of loading or material properties from SHM data is still a challenge because of the finite number of sensors and the large number of potential positions of local failures or disruptions. Numerical algorithms and specific multi-sensor systems should be developed towards this aim.

Within this framework, the main objective of this paper is to propose a methodology to optimize the spatial distribution of embedded sensors used for spatial variability assessment of stationary random fields. Stationary random fields have a stochastic structure and probabilistic properties that could be used to provide rational aid tools for optimizing the number and location of sensors. The assessment of the shape of the Auto-Correlation Function (ACF) is paramount for this spatial variability characterization.

The paper starts in section 2 with a review of key concepts of spatial random field modeling with a focus on stationary random fields. Section 3 describes the proposed method for optimal sensors positioning in order to characterize the spatial correlation structure, illustrated with numerical examples and real measurements on a reinforced concrete (RC) beam (section 4).

2 Main assumptions for the stochastic modeling

In order to simplify the presentation of the proposed methodology, we consider the following main assumptions about the sensors and the random field modeling:

- The stochastic field is considered as: Gaussian, second order stationary, statistically homogeneous and its marginal distribution is known. This assumption implies that less information is required for its characterization.
- Each realization (single trajectory) represents the probabilistic information of all trajectories: mean, variance, spatial correlation. A single trajectory is then sufficient to describe the spatial variability, i.e. the stationary field is ergodic.
- A larger number of discrete sensors can be placed over the same component to characterize both randomness and spatial variability (e.g., from 20 to 60). We consider in this paper long structures with a significant number of sensors (around 200).
- Sensor measurements are considered as ‘perfect’ according to the definition provided in [Schoefs et al., 2009].
- Damage is not affected by the loading or that the effect of loading on the spatial variability can be modelled. Extensions are developed in Schoefs et al. (*under review*).

Several approaches can be used to describe a stochastic field $Z(x,\theta)$ where x denotes the position and θ the hazard: Karhunen-Loève expansion, approximation by Fourier series, EOLE approximation, etc.. This paper uses a Karhunen-Loève expansion to model the stochastic field $Z(x,\theta)$. This expansion represents a random field as a combination of orthogonal functions on a bounded interval.

3 Sensor placement strategy and goals

3.1 Definition of the Spatial Correlation Threshold

The paper focuses on the assessment of the ACF (exponential for example in Eq. (1)) of a stationary field. An optimal geo-positioning of sensors along a trajectory (sampling of the random field) should provide an accurate assessment of the ACF parameters (i.e. b in Eq. (1)) with a limited number of sensors.

$$\rho(\Delta x) = \exp\left(\frac{-\Delta x}{b}\right), 0 < b \text{ and } \Delta x = x_1 - x_2 \quad (1)$$

This exponential ACF will serve r numerical simulations in the following. When looking for the usual shape of a correlation function a regular spacing of sensors could not be optimal. If the distance between two sensors L_b is large, the decay of autocorrelation for short distances cannot be assessed. On the contrary, if L_b is small, there is some information provided for many sensors that will not be useful for the assessment of b . Figure 2 shows that it is possible to install different number of sensors for high and low autocorrelation zones to obtain a good assessment of the autocorrelation parameter by reducing the total number of sensors N_s . The objective is to get a spacing of sensors providing a larger amount of data in the zone of high correlation. However, there is a limited feedback on the autocorrelation function (and consequently the value of b) for defining clearly the high autocorrelation zones. Section 4 presents a sensitivity study about the influence of the a priori knowledge of b .

Let us consider a one-dimensional spatial field. The methodology could be applied on a set of trajectories representing: (i) a set of 1D components (beams), or (ii) a very long 1D-component subdivided artificially or physically (expansion joint or construction joints) in a set of short components, or belonging to a wall structure (steel sheet pile or concrete wall).

In order to limit monitoring costs (number of sensors), we propose to monitor some zones of a trajectory with sensors separated by “sufficiently short distance L_b ” allowing us to assess the shape of the ACF (Eq. (1)) that is

controlled by the parameter b . This “sufficiently short distance” can be seen as an Inspection Distance Threshold (IDT). Thus the non-regular distances of sensors spacing L_b^i should satisfy: $L_b^i \in]0, IDT[$ in the highly correlated zones.

The IDT is defined by assuming that, after a given distance, the events measured from an inspection can be assumed as weakly correlated. A Spatial Correlation Threshold (SCT) defines this weak correlation. For instance, Schoefs et al. (2016) proposed a value $SCT = 0.3$ to get fairly correlated events and $SCT = 0.5$ to get high correlated events. For an exponential ACF, the SCT is linked with IDT by:

$$IDT = -b \cdot \ln(SCT) \quad (2)$$

This paper considers the value $SCT = 0.4$ to determine IDT. For example, for this value of SCT and $b = 1.0$ m, $IDT = 0.67$ m. The effect of this choice is discussed in [Schoefs et al. 2016].

3.2 Parametrization of non regular spacing

In view to reduce the set of potential solutions and simplify the design of the network of sensors, we propose a parameterization. It is based on a division of the trajectory (structural component) into n_p pieces of same size L_m and then a subdivision of each piece into a decreasing N_c^i number of equidistant sensors, with distance L_b^i , following a series according to the octree approach. This approach has the advantage to get more information (more sensors) for small distances between points where the slope of the auto-correlation function must be fitted accurately. The number of sensors in the first piece is computed by:

$$N_c^1 = \text{Round} \left(\frac{N_s}{1 + \sum_{i=2}^{n_p} \frac{1}{2(i-1)}} \right) \quad (3)$$

The number of sensors for the pieces $N_c^2, \dots, N_c^{n_p-1}$ (i.e., N_c^i with $i \in [2; n_p-1]$) is estimated from:

$$N_c^i = \text{Round} \left(\frac{N_c^1}{2(i-1)} \right) \quad (4)$$

The number of sensors for the last piece, $N_c^{n_p}$, is the remaining number of sensors. Knowing the number of sensors in each piece, the distance between sensors in each piece is deduced. To satisfy the condition of sufficient correlation between measurements, we should avoid a distance larger than IDT for the pieces located in the high correlation zone. The length of this zone L_{hc} depends on the autocorrelation parameter b and could be estimated from Eq. (1) by considering a low value of autocorrelation. For example, for $b=1\text{m}$ $L_{hc} \approx -b \ln(0.01) \approx 4.6\text{m}$. However, if $L_b^i > IDT$ for the pieces located in this high correlation zone, the total number of sensors, N_s , should be increased until ensuring this condition for a given number of pieces.

3.3 Parameter estimation, sensitivity analysis and optimization

Stationary stochastic fields are simulated by the Karhunen-Loève expansion assuming an exponential ACF (Eq. (1)), whose parameter b has to be identified by knowing the two first statistic moments (μ_Z, σ_Z). Based on a continuous trajectory, for fixed values of N_s and n_p , we obtain a sample of discrete realizations from the sensor measurements $\hat{Z} = \{z_1, z_2, \dots, z_{N_s}\}$ corresponding to the sensors positions $X = \{x_1, x_2, \dots, x_{N_s}\}$ following the discretization procedure presented in previous section. We assess the value of b by using the Maximum Likelihood Estimate method (MLE), reported by Li (2004). To account for the effect of random shape of trajectories, the analysis is carried out over a database containing 10,000 trajectories generated by Monte-Carlo simulations. This allows estimating 10,000 values \hat{b} for each distribution of the sensor – i.e. one set of the couple (N_s, n_p) . We select in this paper a confidence interval of the mean $\mu_{\hat{b}}$ expressed as a percentage Δ of the theoretical (true) value b^{th} to evaluate the quality of the SHM. From the 10,000 Monte-Carlo simulations we estimate the bounds of the confidence interval and the probability $P_{I,b}$ to get values inside the confidence interval, from the monitoring data. In a reliability study, $P_{I,b}$ will be discussed according to the requirements on the accuracy of the probability of failure assessment [Stewart, 2006]. Thus we focus on the quality estimator:

$$P_{I,b} = P(\mu_{\hat{b}} \in [(1 - \Delta)b^{th}, (1 + \Delta)b^{th}]) \quad (5)$$

where $\mu_{\hat{b}}$ is the mean value of \hat{b} computed from 10,000 Monte-Carlo simulations. We define another estimate ε_b , the normalized quadratic error of the parameter \hat{b} :

$$\varepsilon_b = \left(\frac{\hat{b} - b^{th}}{b^{th}} \right)^2 \quad (6)$$

Finally, the optimal position and number n_p^{opt} of sensors is obtained by:

$$n_p^{opt} = \underset{n_p}{\text{Argmax}}\{P_{I,b}(N_s)\} \quad (7)$$

4 Numerical simulations and real study case

4.1 Application to a numerical study case

For illustrating the methodology and generalization purposes, it is considered in the following sections a set of 1D-components (beams) with a very large total length $L \gg b$. The case of components with a limited size is discussed in (Schoefs et al., *under review*) excepting those where $L < L_b$ for which it is theoretically impossible to identify fully the stochastic field. The Gaussian stationary stochastic field is characterized by: $b_{th}=1\text{m}$, $IDT=0.91\text{m}$ from Eq. (2), $\mu_Z = 100$ and $\sigma_Z = 20$. The objective is to optimize the position of sensors in view to reach a good assessment of b for an error $\Delta = 10\%$. We first analyze the effect of the number of pieces (n_p) on the quality of assessment defined according to Eq. (5) for a large number of sensors N_s and large length L ; namely $N_s=200$ and $L=100\text{m}$. We vary the number of pieces from 1 (200 sensors equally separated by the distance $L_b = IDT$) to 20 (72, 36, 18, 12, 9, 7, 6, 5, 5, 4, 4, 3, 3, 3, 3, 2, 2, 2, and 2).

Figure 1a presents the evolution of the quality estimator ($P_{I,b}$) with n_p for 10,000 simulated trajectories.

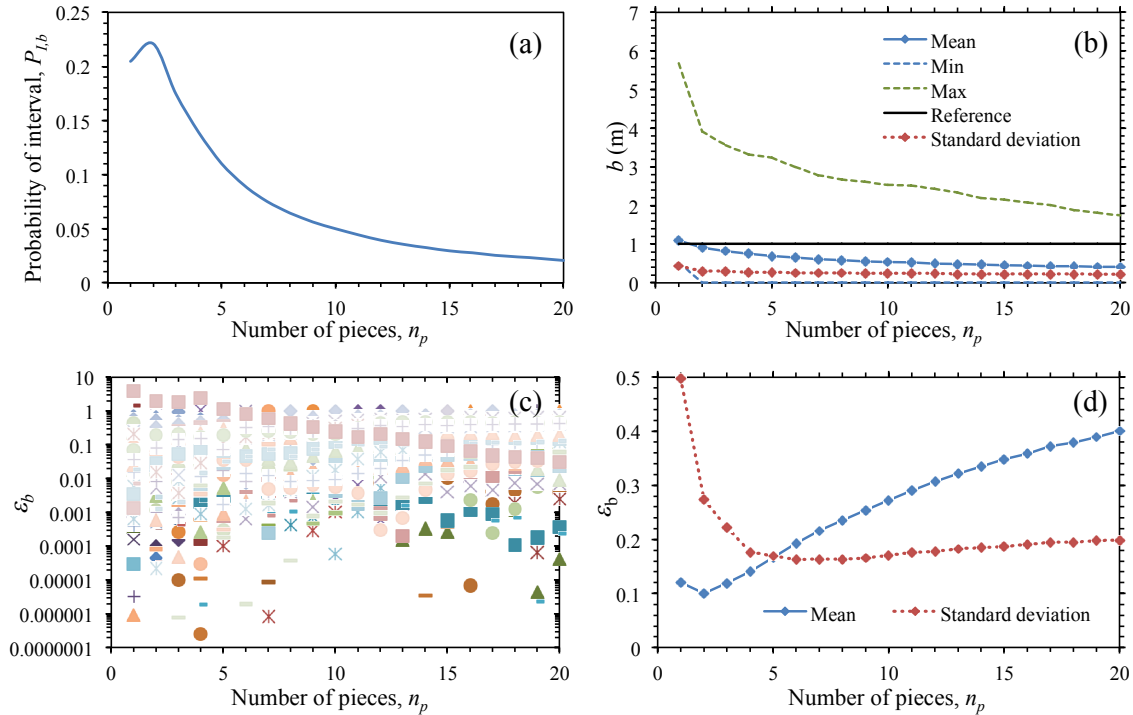


Fig. 1. Effect of number of pieces n_p on:
 a - the probability of interval $P_{I,b}$; b - the estimated values of b
 c - the distribution of ε_b ; d - the mean and standard deviation of ε_b ($N_s=200$, $L=100\text{m}$ and $\Delta=10\%$)

The regular spacing obtained for $n_p=1$ is shown to be not optimal whereas the optimum is found for $n_p=2$ with 133 sensors spaced 37.8 cm in the first piece of 50m and 67 sensors with spacing equal to 74.6cm in the second piece. Figure 1 presents other results to improve the understanding of the causes of this trend. Figure 1b plots the evolution with n_p of the two first statistics (mean and standard deviation) and the minimum and maximum values obtained for b from a sample of size 10,000. It is observed that the mean value decreases slightly with n_p and becomes stable with a significant bias in comparison to the reference theoretical value (1m). This means that identification algorithm underestimates the value of b . Thus, even if the standard deviation decreases with n_p , $P_{I,b}$ is not optimal for high values of n_p . Note that the maximum and minimum bounds are not symmetrical to the mean; that is due to the non-symmetrical distribution of b for a fixed sensor distribution. Figure 1c presents the potential relative error ε_b that can reach 4.8 (near 500%) for one realization upon 10,000. The results on Figure 1d show the mean and standard deviation of ε_b and confirm that the error on the mean governs the level of the quality estimator $P_{I,b}$ where the minimum value of the mean error is obtained for $n_p=2$. Figure 1d also indicates that there is a significant reduction of the standard deviation of the error from $n_p=1$ to 2.

We focus now on the effect of small perturbations around the value of b on the optimal solution. This is a key issue for studying the robustness of the solution obtained from an *a priori* value of b . This sensitivity analysis studies the effect of b on the error ε_b by assuming that b takes the following values around the reference one (i.e., $b=1m$): 0.8, 0.9, 1, 1.1, and 1.2 m (Figure 2).

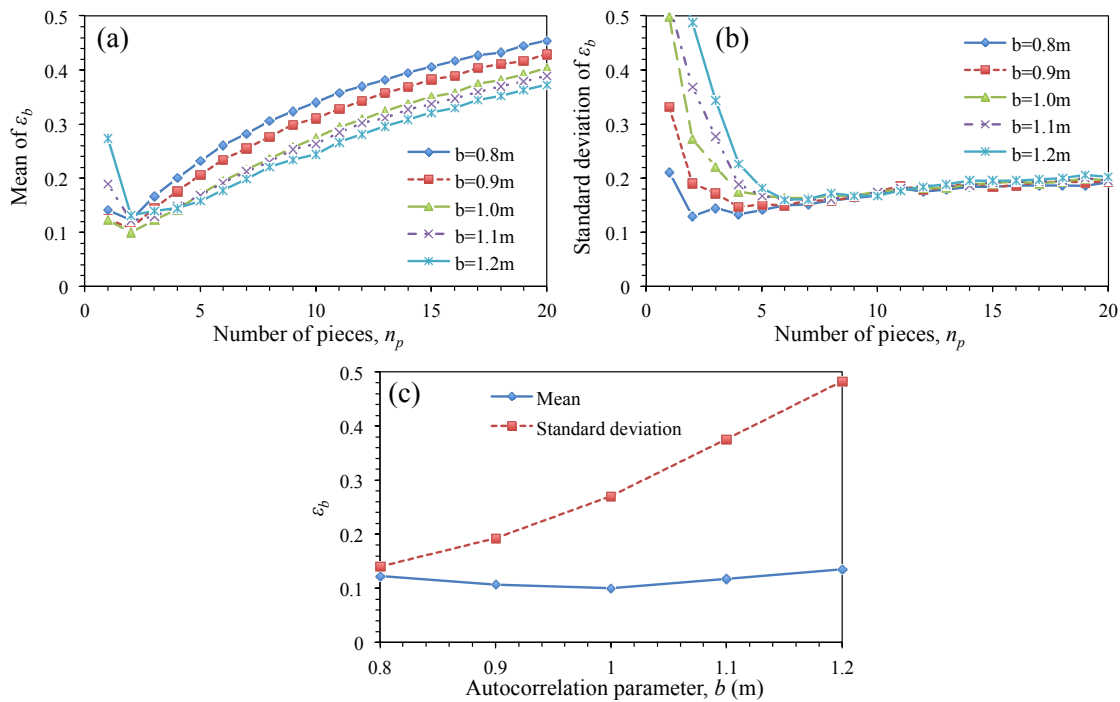


Fig. 2. Sensitivity of ε_b for:
a - the mean of ε_b ; b - the standard deviation of ε_b
c - the mean and standard deviation of ε_b for $n_p=2$ ($N_s=200$, $L=100m$)

Figure 2a plots the mean of the error ε_b for various values of n_p and b . It is found that the minimum error corresponds to $n_p=2$ for all values of b . Figure 2b shows that the standard deviation of the error is sensitive to b for $n_p=2$ and that leads to a given value for $n_p > 5$. Figure 2c presents the mean and standard deviation of the error for $n_p=2$. It is noted that the error on the mean is almost constant with a minimum for $b=1m$ but the error on the standard deviation increases with b . It is possible to conclude from this trend that under-estimating slightly the value of b reduces the error.

The cases of small structures or small number of sensors are available in Schoefs et al. (*under review*).

4.2 Illustration for a real study case

The authors applied the proposed methodology and previous findings to two study cases for which real spatially distributed data are available (Schoefs et al., *under review*). We consider in this paper only one of them, the

inspection of the water content along a 16m length reinforced concrete beam placed on the site of IFSTTAR Laboratory, Nantes, France [Schoefs et al., 2016]. The measurements were carried out by using a capacitive NDT tool.

Figure 3a presents the spatial measurements (trajectory) of the water content (RC beam). Mean and standard deviation are: $\mu_W = 6.3\%$, $\sigma_W = 0.67\%$ for the RC beam (computed from a sample of 80 measures every 20 cm).

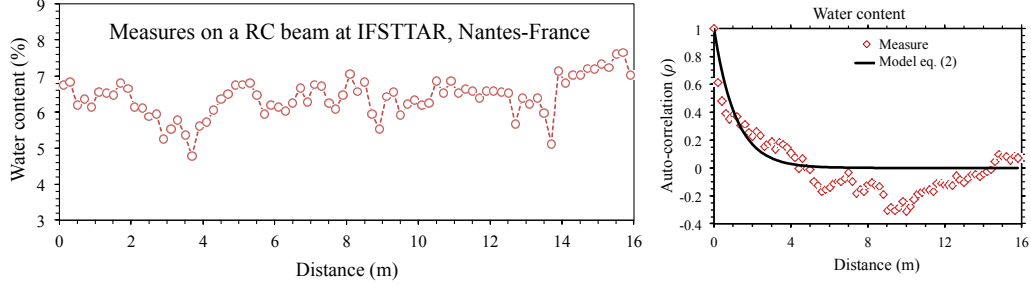


Fig. 3. a- Experimental trajectories of water content; b- auto-correlation data and fitted ACFs for water content in a RC beam (IFSTTAR, Nantes, France)

Figure 3b presents the computed autocorrelation values. We obtain a classical shape including negative values [henari & Dodaran, 2010]. Applying the procedure described previously it was found that the exponential correlation functions are appropriate to model the empirical values. The following parameter of the autocorrelation function (Eq. (1)) were estimated: $b_W = 0.42\text{m}$ assumed in the following results and discussions as the theoretical value. Based on the fitted auto-correlation functions, the Inspection Distance Thresholds (IDT) is: $IDT_W = 0.5\text{m}$. Taking into account the length of the structural components and the findings of Schoefs et al. (*under review*), we propose a regular spacing of measurements for the RC beam because the ratio $IDT_W/L = 0.4/16 > 1/40$. In the following we compare real and numerical estimations to determine the appropriateness of the proposed sensor spacing in each case.

We estimate the errors on the identification of ε_b for both real data and simulations for the two study cases. Numerical simulations are based on: (i) the procedures to generate trajectories, and (ii) the values of mean, standard deviation and autocorrelation parameter identified upon. The main goal of this section is to validate the proposed numerical approach as well as to verify if the practical recommendations of the previous numerical findings could be applied to real measures.

Figure 4a compares the evolution of the error of the assessment of b by considering various n_p for results obtained from simulations and those computed from real data measured on the RC beam. The numerical mean as well as the minimum and maximum values were computed from 10,000 simulations.

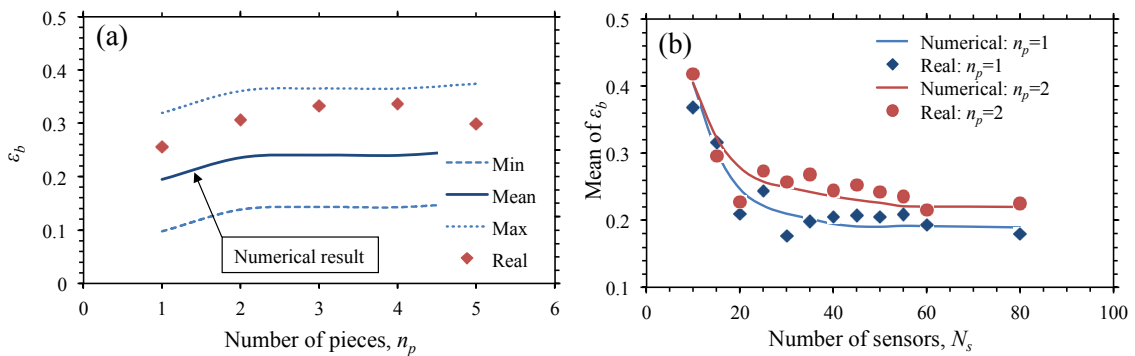


Fig. 4. Comparison between simulated results and real inspection values in the case of water content (RC beam, $L = 16$ m, $IDT = 0.4\text{m}$):

a - effect of n_p on ε_b , for $N_s = 40$ sensors; b - effect of N_s on the mean of ε_b

The results show that the numerical and mean values are close and that ε_b is minimum for $n_p = 1$. This behavior confirms the recommendation based on the numerical findings for the case of $L < 40IDT$ where the regular spacing is suggested in such a case. Figure 4b compares the evolution of the mean of ε_b with N_s for $n_p = 1$ and $n_p = 2$. It is observed that the mean of ε_b decreases when more information from additional sensors is considered.

There is a convergence in the error that is faster when $n_p=1$; in such a case it is reached for $N_s > 30$ sensors. The results also show that a regular spacing with $n_p=1$ leads to lower error for both simulated and real data.

5 Conclusion

This paper proposed an original method for defining a non-regular spacing of sensors devoted to the assessment of the autocorrelation function parameter of stationary fields. The method is based on the probabilistic identification of the autocorrelation function parameter and aims at reducing the error on its estimation. Numerical simulations of Gaussian stationary stochastic fields illustrate the potential of the method by providing a decision aid tool when a limited number of sensors is available. Based on these numerical results, it was found that the position of sensors is a key factor for estimating the autocorrelation function parameter.

The paper shows also the important role of the position of sensors in the estimation of the autocorrelation function parameter on a real study case (concrete beam).

Acknowledgements

The authors would like to acknowledge the Pays de la Loire Region for supporting the projects ECND-PdL and SI3M as well as the European commission for funding the DuratiNet EC Interreg project (<http://www.duratinet.org>).

References

- Chenari RJ, Dodaran RO. New method for estimation of the scale of fluctuation of geotechnical properties in natural deposits. *Computational Methods in Civil Engineering* 2010;1:55–66.
- Li Y. Effect of spatial variability on maintenance and repair decisions for concrete structures. Delft University, Delft, Netherlands, 2004.
- Li J, Masia MJ, Stewart MG, Lawrence SJ. Spatial variability and stochastic strength prediction of unreinforced masonry walls in vertical bending. *Engineering Structures* 2014;59:787–97. doi:10.1016/j.engstruct.2013.11.031.
- Srivastava A. Spatial Variability Modelling of Geotechnical Parameters and Stability of Highly Weathered Rock Slope. *Indian Geotechnical Journal* 2012;42:179–85.
- Gomez-Cardenas C, Sbartaï ZM, Balayssac JP, Garnier V, Breyse D. New optimization algorithm for optimal spatial sampling during non-destructive testing of concrete structures. *Engineering Structures* 2015;88:92–9. doi:10.1016/j.engstruct.2015.01.014.
- Griffiths DV, Fenton GA. Influence of soil strength spatial variability on the stability of an undrained clay slope by finite elements. *Slope Stability 2000 ASCE* 2000:184–93.
- Hu W-H, Thöns S, Rohrmann RG, Said S, Rucker W. Vibration-based structural health monitoring of a wind turbine system. Part I: Resonance phenomenon. *Engineering Structures* 2015;89:260–72. doi:10.1016/j.engstruct.2014.12.034.
- Kulprapha N, Warnitchai P. Structural health monitoring of continuous prestressed concrete bridges using ambient thermal responses. *Engineering Structures* 2012;40:20–38. doi:10.1016/j.engstruct.2012.02.001.
- O'Connor A, Kenshel O. Experimental Evaluation of the Scale of Fluctuation for Spatial Variability Modeling of Chloride-Induced Reinforced Concrete Corrosion. *Journal Of Bridge Engineering* 2013;18:3–14.
- Nguyen NT, Sbartaï Z-M, Lataste J-F, Breyse D, Bos F. Assessing the spatial variability of concrete structures using NDT techniques – Laboratory tests and case study. *Construction and Building Materials* 2013;49:240–50. doi:10.1016/j.conbuildmat.2013.08.011.
- Nguyen NT, Sbartaï ZM, Lataste J-F, Breyse D, Bos F. Non-destructive evaluation of the spatial variability of reinforced concrete structures. *Mechanics & Industry* 2014;16:103. doi:10.1051/meca/2014064.
- Pasqualini O, Schoefs F, Chevreuil M, Cazuguel M. Measurements and statistical analysis of fillet weld geometrical parameters for probabilistic modelling of the fatigue capacity. *Marine Structures* 2013;34:226–48. doi:10.1016/j.marstruc.2013.10.002.
- Schoefs F, Clement A, Nouy A. Assessment of spatially dependent ROC curves for inspection of random fields of defects. *Structural Safety* 2009;31:409–19.
- Schoefs F, Bastidas-Arteaga E, Tran TV, Villain G, Derobert X. Characterization of random fields from NDT measurements: A two stages procedure. *Engineering Structures* 2016;111:312–22. doi:10.1016/j.engstruct.2015.11.041.
- Schoefs F., Bastidas-Arteaga E., Tran T.V., Optimal Embedded Sensor Placement for Spatial Variability Assessment of Stationary Random Fields, *Engineering Structures*, under review.
- Stewart MG. Spatial variability of pitting corrosion and its influence on structural fragility and reliability of RC beams in flexure. *Structural Safety* 2004;26:453–70.
- Stewart MG. Spatial Variability of Damage and Expected Maintenance Costs for Deteriorating RC Structures. *Structure and Infrastructure Engineering* 2006;2:79–96.